ELSEVIER

Journal of Alloys and Compounds 408–412 (2006) 1373–1376

Journal of ALLOYS AND COMPOUNDS

www.elsevier.com/locate/jallcom

Corrosion assessment of Nd–Fe–B alloy with Co addition through impedance measurements

Satoshi Sunada [a,*], Kazuhiko Majima [a], Yasuhiro Akasofu [a], Yuji Kaneko [b]

[a] *Department of Material System Engineering and Life Science, Faculty of Engineering, Toyama University, Gofuku 3190, Toyama 930-8555, Japan*
[b] *Neomax Co. Ltd., 2-15-17 Egawa, Shimamoto-cho, Mishima-gun, Osaka 618-0013, Japan*

Available online 8 June 2005

Abstract

Effect of Co addition on improving the corrosion resistance of $Nd_{11.8}Fe_{82.3-x}Co_xB_{5.9}$ specimens with different x ($x = 0$, 2.5, 5.0, 7.5, 10.0) have been investigated through the electrochemical method including the impedance measurement. With increasing amount of Co content the natural electrode potential shifted to nobler side. The Nyquist plot showing a semi circle in which frequency increases in counter clockwise direction was obtained. From the result it was clarified that the diameter of the semi circle corresponding to the charge transfer resistance, R_{ct}, became larger with increasing Co content, which indicates the improvement of the corrosion resistance for the $Nd_{11.8}Fe_{82.3-x}Co_xB_{5.9}$ specimens by Co addition because the R_{ct} is inversely proportional to the corrosion rate. Judging from these results it is suggested that the impedance measurement is one of the effective methods to obtain the information of corrosion behavior for the $Nd_{11.8}Fe_{82.3-x}Co_xB_{5.9}$ specimens.

Keywords: Nd-Fe-B magnet; Corrosion resistance; Nyquist plot; Charge transfer resistance; Immersion test

1. Introduction

It is well known that permanent magnets based on intermetallic compounds composed of rare earth elements and transition metals exhibit exceptionally excellent magnetic properties. Therefore, they have been in practical use for numerous applications such as devices in consumer electronics, computer peripherals, acoustics, magnetic resonance, biomedical and automation. Among these magnets, particularly the Nd–Fe–B magnet, the world strongest magnet, exhibits a maximum energy product $(BH)_{max}$ higher than 350 kJ/m^3, and hence, it occupies a leading position today. However, it is at the same time notorious for its poor corrosion resistance [1–4]. The corrosion causes surface degradation and thereby deteriorates the magnetic properties significantly. Generally, the Nd–Fe–B permanent magnet has been produced by the liquid phase sintering process according to the liquidus line in Nd–Fe–B ternary phase diagram [5]. As a result, this magnet is composed of the matrix phase of $Nd_2Fe_{14}B$ (2–14–1 phase), and the grain boundary phases of non-magnetic $Nd_{1.1}Fe_4B_4$ (boron-rich phase) and Nd-rich phase. Therefore, it is necessary to investigate the corrosion behavior of these phases individually.

It has been reported that the corrosion resistance improved by the Co addition [6], yet not much has been studied on corrosion mechanism of Nd–Fe–B ternary magnets. What has been investigated so far is its corrosion resistance by acceleration tests in atmosphere near the actual conditions used as manufacturing products. In this study, the specimens corresponding to main phase of $Nd_{11.8}Fe_{82.3-x}Co_xB_{5.9}$ (2–14–1 phase) with different x were prepared and their corrosion behavior was studied by the electrochemical method including the impedance method.

2. Experimental

In this study, using neodymium metal (99.5% of purity), electrolytic iron (99.9% of purity), Co (99.9% of purity) and boron (99.9% of purity), the alloys corresponding to $Nd_{11.8}Fe_{82.3-x}Co_xB_{5.9}$ (2–14–1 phase) with different x ($x = 0$, 2.5, 5.0, 7.5, 10.0) were prepared by using a high-frequency induction furnace, and then they were homogenized at 1353 K

* Corresponding author.
E-mail address: suna@eng.toyama-u.ac.jp (S. Sunada).

0925-8388/$ – see front matter © 2005 Elsevier B.V. All rights reserved.
doi:10.1016/j.jallcom.2005.04.039

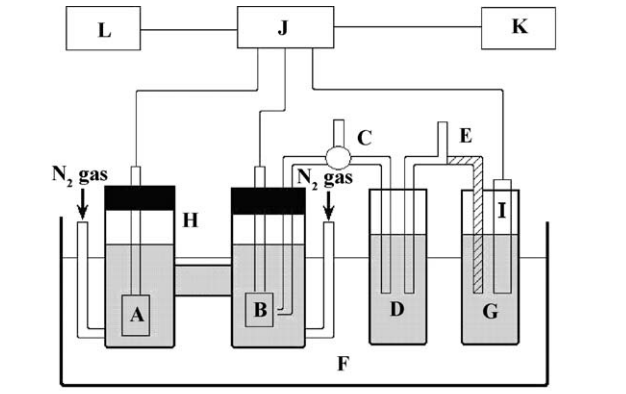

Fig. 1. Schematic diagram of apparatus for impedance measurement.

for 21.6 ks. The constituent phases were identified by X-ray diffraction and EPMA, and it was confirmed that all of $Nd_{11.8}Fe_{82.3-x}Co_xB_{5.9}$ alloys were composed of single phase irrespective of x. Electrochemical methods were conducted as follows. The specimen with the dimension of 50 mm in length, 15 mm in width and 2 mm in thickness was polished with No. 2000 grit water-proofed abrasive paper followed by washing in alcohol and subsequent ultrasonic rinsing in acetone. The specimen electrode was coated with silicon rubber leaving uncoated area of 15 mm × 5 mm. Testing solution should be prepared considering that the specimen described above has poor corrosion resistance. In our experiment, therefore, 2.5% Na_2SO_4 aqueous solution of pH 6.4 was used, in which the solution was adjusted by deionized water whose specific electrical conductivity was less than 2.0×10^{-5} S m. The schematic diagram of apparatus for impedance measurement is shown in Fig. 1. It consists of thermostatic bath, H-type electrolytic cell with anodic and cathodic chambers of 2×10^{-4} m^{-3} in volume, intermediate cell Ag-AgCl (3.33 kmol/m^3 KCl) as a reference electrode, potentiostat, AC impedance meter and a personal computer for the measurement control. A natural electrode potential with perturbation ac potential, amplitude of which was 10 mV, was applied to the specimen in ac impedance measurements. Analyzing frequency range was from 10 mHz to 100 kHz. All of the potential values were shown based on the Ag-AgCl reference electrode. The immersion test was conducted in deionized water whose specific electrical conductivity was less than 2.0×10^{-5} S m and 0.176 kmol/m^3 Na_2SO_4 aqueous solution under the condition of air-bubbling. The specimens were kept in the deionized water for 86.4 ks or in the Na_2SO_4 aqueous solution for 7.2 ks. After the immersion test, metal elements dissolved in each solution were determined by ICP (Inductively coupled plasma) and the relation between mass of dissolved element and additional Co content was obtained.

3. Results and discussion

Fig. 2 shows the effect of Co addition on the natural electrode potential of $Nd_{11.8}Fe_{82.3-x}Co_xB_{5.9}$ specimens with different x (x = 0, 2.5, 5.0, 7.5, 10.0), where the natural potential was obtained from potentiodynamic polarization curves. With an increase of the substitution amount of Co the natural electrode potential shifts to nobler side, which indicates the enhancement of corrosion resistance. The four reactions: $Nd \rightarrow Nd^{3+} + 3e^-$, $Fe \rightarrow Fe^{2+} + 2e^-$, $Co \rightarrow Co^{2+} + 2e^-$ and $B \rightarrow B^{3+} + 3e^-$ are considered as anodic reactions for the $Nd_{11.8}Fe_{82.3-x}Co_xB_{5.9}$ (x = 0, 2.5, 5.0, 7.5, 10.0) specimens. Since these $Nd_{11.8}Fe_{82.3-x}Co_xB_{5.9}$ (x = 0, 2.5, 5.0, 7.5, 10.0) specimens differ one another in both Fe and Co content, it is considered that the natural electrode potential of them depends on the amount of Fe and Co content. The standard oxidation–reduction (redox) potential values of Fe and Co are represented as follow:

$$Fe \rightarrow Fe^{2+} + 2e^- \quad (-0.440\,V_{SHE})$$

$$Co \rightarrow Co^{2+} + 2e^- \quad (-0.277\,V_{SHE})$$

Comparison of the standard redox potentials suggests that corrosion propagation is less in Co than in Fe. Therefore, it is considered that the Co addition suppresses the anodic reaction and shifts the natural electrode potential of 2–14–1 phase to the nobler side. Besides the potentiodyamic polarization curve, the impedance measurement is also the effective and informative method to clarify corrosion behavior. The impedance feature of each specimen is expressed as the relation between imaginary component Z (Im Z) and

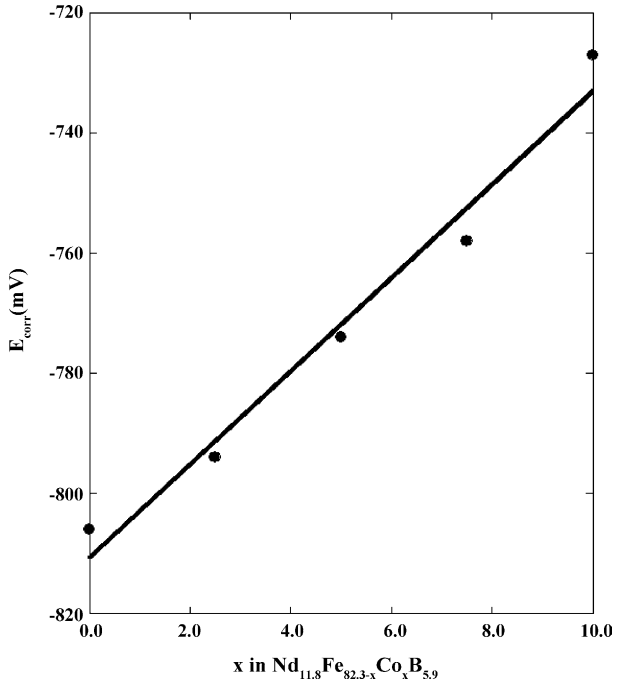

Fig. 2. Effect of Co content on E_{corr} for $Nd_{11.8}Fe_{82.3-x}Co_xB_{5.9}$ (x = 0, 2.5, 5.0, 7.5, 10.0) specimens.

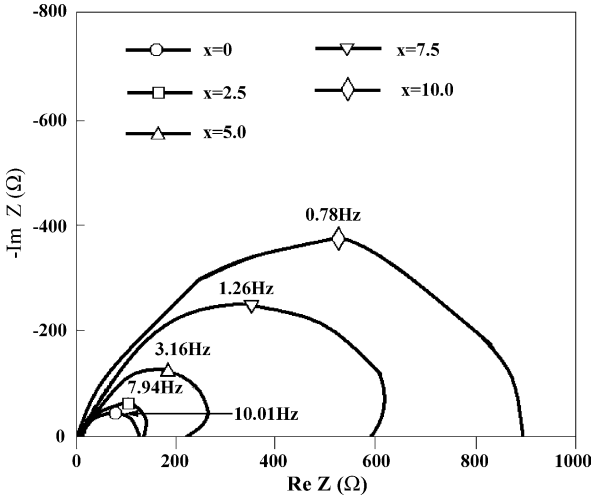

Fig. 3. Nyquist diagrams of $Nd_{11.8}Fe_{82.3-x}Co_xB_{5.9}$ ($x = 0$, 2.5, 5.0, 7.5, 10.0) specimens.

real component Z (Re Z) in Nyquist plots, where $\omega = 2pF$. Fig. 3 shows the Nyquist plots for the $Nd_{11.8}Fe_{82.3-x}Co_xB_{5.9}$ ($x = 0$, 2.5, 5.0, 7.5, 10.0) specimens. The Nyquist plots show a semi circle in which frequency increases in counter clockwise direction. At the highest frequency, Im Z disappears leaving only the solution resistance, R_{sol}. At the lowest frequency, Im Z again disappears leaving a sum of R_{sol} and the charge transfer resistance, R_{ct}. Here, the R_{ct} is inversely proportional to the corrosion rate. As may be seen in Fig. 4 presenting the Co content dependence of R_{ct} for the $Nd_{11.8}Fe_{82.3-x}Co_xB_{5.9}$ ($x = 0$, 2.5, 5.0, 7.5, 10.0) specimens, the value of R_{ct} increased with increasing amount of the additional Co, which shows the improvement of the corrosion resistance for the $Nd_{11.8}Fe_{82.3-x}Co_xB_{5.9}$ specimens by Co addition. Fig. 5 shows the immersion test in 0.176 kmol/m^3 Na_2SO_4 aqueous solution of pH 6.4 for 7.2 ks. After the immersion test, metal elements dissolved in each solution were determined by ICP. The dissolved amounts of Fe and B decreased with increasing amount of additional Co content. Though the slight increment of the dissolved Nd is observed in the case of 2.0 wt.% Co content, the similar decreasing tendency of the dissolved Nd is recognized with increasing Co content as a whole. These tendencies were also observed in the immersion test in deionized water whose specific electrical conductivity was less than 2.0×10^{-5} S m. Fig. 6 shows the mass of total dissolve after immersion test. Both of the total dissolves in the deionized water and 0.176 kmol/m^3 Na_2SO_4 aqueous solution decreased with increasing amount of Co content, and the amount of the total dissolve in the former solution was less than that in the latter solution. This is because the ionic conductivity in the former solution is lower than that in the latter solution. These experimental results in Figs. 5 and 6 well correspond to those of the impedance measurements in Figs. 3 and 4, which suggests that the impedance measurement gives the important information for the corrosion behavior of $Nd_{11.8}Fe_{82.3-x}Co_xB_{5.9}$ specimens. Though the impedance measurement in this experiment was conducted at the natural electrode potential with a perturbation ac potential, amplitude of which was 10 mV, it should be performed at the other potential than the natural electrode potential in the future to obtain much more corrosion information on the $Nd_{11.8}Fe_{82.3-x}Co_xB_{5.9}$ specimen.

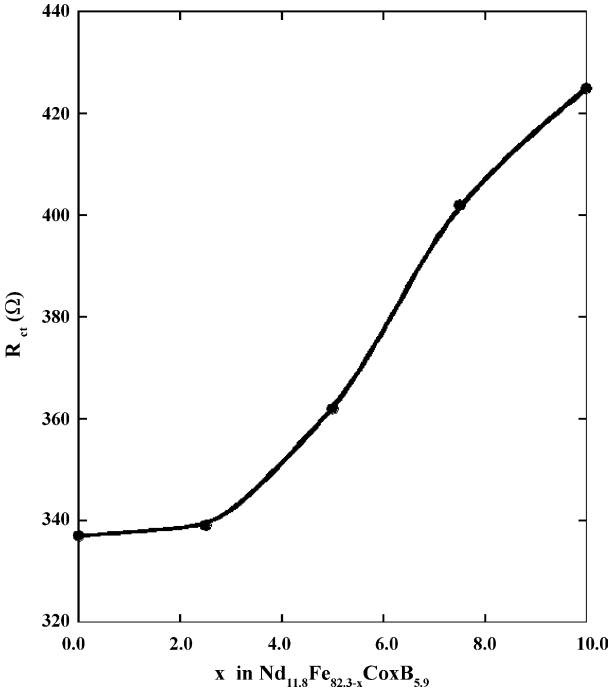

Fig. 4. Effect of Co content on R_{ct} of $Nd_{11.8}Fe_{82.3-x}Co_xB_{5.9}$ ($x = 0$, 2.5, 5.0, 7.5, 10.0) specimens.

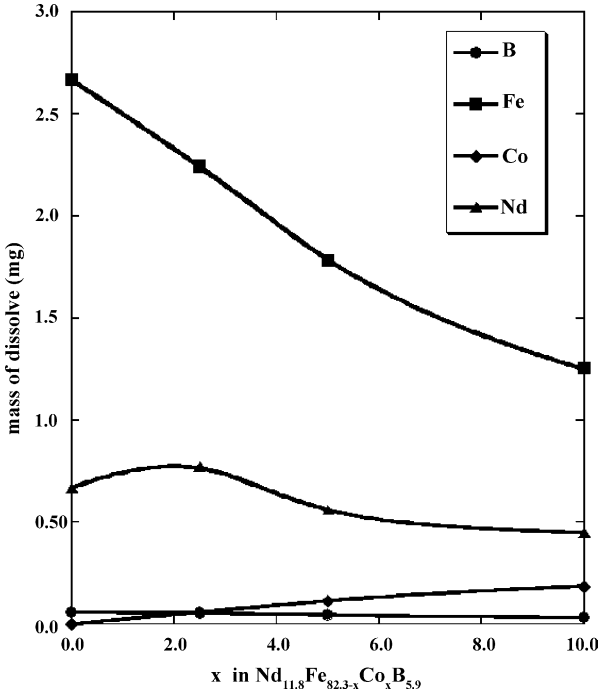

Fig. 5. Mass of dissolves vs. x curves after immersion test in 0.176 kmol/m^3 Na_2SO_4 for $Nd_{11.8}Fe_{82.3-x}Co_xB_{5.9}$ ($x = 0$, 2.5, 5.0, 10.0) specimens.

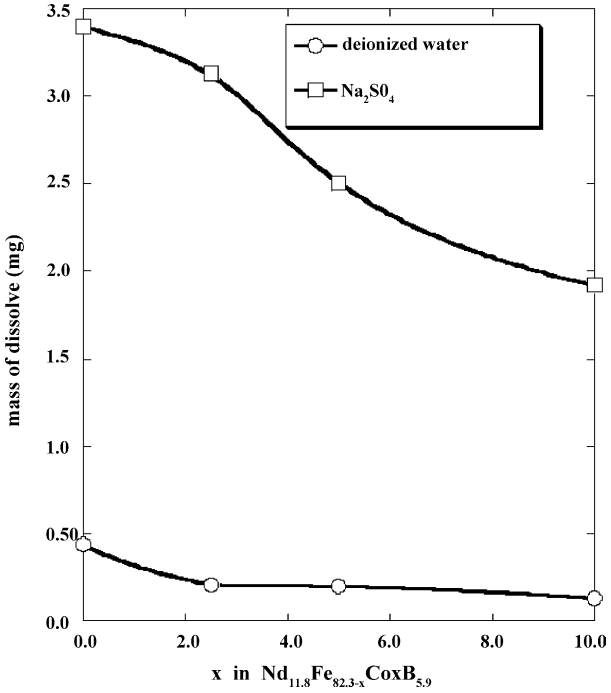

Fig. 6. Mass of total dissolves vs. x curves for $Nd_{11.8}Fe_{82.3-x}Co_xB_{5.9}$ ($x = 0$, 2.5, 5.0, 10.0) specimens.

4. Conclusion

In this experiment, the effect of Co addition on the corrosion behavior of the $Nd_{11.8}Fe_{82.3-x}Co_xB_{5.9}$ alloys was investigated by the electrochemical method, and the results obtained are summarized as follows:

(1) The potentiodynamic curves showed that the natural electrode potential shifted to nobler side with increasing amount of Co content for $Nd_{11.8}Fe_{82.3-x}Co_xB_{5.9}$ alloys.
(2) The Nyquist plots indicated that the charge transfer resistance, R_{ct}, increased with increasing amount of Co content for $Nd_{11.8}Fe_{82.3-x}Co_xB_{5.9}$ alloys.
(3) The immersion test showed that both of the total dissolves in the deionized water and 0.176 kmol/m^3 Na_2SO_4 aqueous solution decreased with increasing amount of Co content, and the amount of the total dissolve in the former solution was less than that in the latter solution.

Acknowledgement

The authors are grateful to Takahashi Industrial and Economic Research foundation for their financial contribution.

References

[1] P. Mitchell, IEEE Trans. Magn. 26 (1990) 1993.
[2] H. Bala, M.A. Malik, S. Szymura, K. Ohashi, J. Alloys Compd. 217 (1995) 268.
[3] L. Shultz, A.M. El-Aziz, G. Barkleit, K. Mummert, Mater. Sci. Eng. A 267 (1999) 307.
[4] A.M. El-Aziz, A. Kirchner, O. Gutfleisch, A. Gebert, L. Shultz, J. Alloys Compd. 311 (2000) 13.
[5] K. Majima, Y. Kaneko, S. Katsuyama, H. Nagai, Mater. Trans. JIM 35 (1994) 473.
[6] K. Ohashi, Y. Tawara, T. Yokoyma, N. Kobayashi, Proceedings of the Ninth International Workshop on Rare Earth Magnets and their Applications, 1987, p. 355.